Synthesis of White Mineral Trioxide Aggregate (WMTA) Using Silica from Rice Husk and Calcium Carbonate from Limestone

Anwar Jaman [a,*], Muhammad Ulin Nuha ABA [b], Oksita Asri Widyayanti [c]

[a] Department of Pharmacy, Mitra Karya Mandiri Polytechnic, Brebes, Central Java, Indonesia
[b] Department of Electromedical Engineering, Bina Trada Polytechnic, Semarang, Central Java, Indonesia
[c] Department of Medical Laboratory Technology, Yakpermas Polytechnic, Banyumas, Central Java, Indonesia

* Corresponding author: anwar.jaman@gmail.com

Article Info

Abstract

White Mineral Trioxide Aggregate (WMTA) was produced using silica as the initial material extracted from rice husk ash and calcium carbonate limestone. This research was initiated by calcinating rice husk ash at 700°C for 3 hours. Silica extraction was performed using 2 M NaOH and added HCl. The extract precipitate was washed using deionized water. Calcium carbonate was made from limestone using 1 M HNO_3 and NH_3 and continued with carbonation. WMTA was produced by mixing SiO_2, $CaCO_3$, and Al_2O_3. The mixture was homogenized with deionized water and heated, then pellets calcined made at a temperature of 1000°C, and calcination products were added Bi_2O_3. Synthesized WMTA characterized using TGA/DSC, FTIR, and XRD showed the presence of Ca_3SiO_5, Ca_2SiO_4, and $Ca_3Al_2O_6$ phases, which were like ProRoot's WMTA.

1. Introduction

Silica and calcium carbonate are the constituent components of MTA, which are widely used as dental bio-cement materials. These materials are used as restorative materials to line the roots of teeth, cover small holes in teeth, and reduce the occurrence of apexogenesis and hypersensitivity in teeth [1]. MTA is one of the most widely used fillings and endodontic treatment materials. Unal et al. [2] stated that MTA has biocompatibility, excellent sealing ability, radiopacity, and moisture resistance. MTA material has the potential to induce cementogenesis and osteogenesis in filling the hollow internal root resorption areas during the apical root canal treatment process [3].

One of the most often used materials in endodontic therapy is MTA. Many minerals, such as tricalcium oxide, silica oxide, tricalcium silicate, tricalcium aluminate, and dicalcium silicate, are present in this substance. MTA also contains 5% hydrated calcium sulphate and tetra calcium aluminoferrite, as opposed to MTA ProRoot, which typically comprises 70% Portland cement, 20% bismuth oxide, and 5% gypsum [4]. MTA is available in two different product types on the market: grey mineral trioxide aggregate (GMTA) and mineral trioxide aggregate (WMTA). GMTA has the problem of discoloring the tissues around the teeth due to its high Fe concentration [5]; hence, WMTA is the most recent product to replace GMTA [6].

Commercial MTA is relatively expensive, around 80-85 USD per gram, so it becomes one of the problems in endodontic treatment in Indonesia. The vast majority of endodontic materials utilized are imported. Due to the lengthy delivery process, imported products are susceptible to having a shorter shelf life. The shelf life of endodontic supplies may be shorter in humid environments. Based on these issues, it is required to commence the production of MTA endodontic materials with adequate properties using basic ingredients readily available in Indonesia; this would make the products more affordable and extend their shelf life.

Limestone, an abundant mineral resource in Indonesia spread across various islands such as Sumatra, Java, Nusa Tenggara, Sulawesi, Papua, and other islands, is estimated at around 2,160 billion tons [7]. Recent uses of limestone are limited to quicklime and cement industry raw materials; hence, its economic value is modest. Conversely, limestone is utilized as a WMTA

precursor because it includes a high concentration of calcium carbonate ($CaCO_3$), roughly 95% [8].

Rice husks are generally considered agricultural waste resulting from the rice milling process. In the rice milling process, about 20-30% rice husk is obtained, and about 14-20% ash is produced from burning rice husk. The main components of rice husk are cellulose (25 to 35%), hemicellulose (18 to 21%), lignin (26 to 31%), and silica (15 to 17%), In rice husk, there is about 15-20% silica, or about 85-95% silica is present in rice husk ash from complete combustion [9]. Therefore, the natural material silica from rice husk ash can be used as a precursor for the manufacture of WMTA.

Based on this description, this study examines the manufacture of White Mineral Trioxide Aggregate (WMTA) by utilizing natural silica materials from rice husks and calcium carbonate from limestone using the calcination method, which will form aggregates between silica and calcium carbonate so that it will have characteristics with WMTA commercial (ProRoot), as determined by DTA/TGA, XRD, FTIR, and SEM analysis.

2.   Experiments

2.1.   Materials and Instruments

The materials were rice husk, limestone, NaOH, 37% HCl, NaOH, HNO_3, 25% NH_3, distilled water, CO_2 gas, synthesized calcium carbonate, Al_2O_3, Bi_2O_3. The instruments were Thermogravimetric Analysis (TGA), Differential Scanning Calorimetry (DSC), X-Ray Diffraction (XRD), Fourier Transform Infrared Spectroscopy (FTIR), and Scanning Electron Microscopy (SEM).

2.2.   Preparation and Extraction of Rice Husk Silica

Rice husk was burned to charcoal for 2-3 hours, thinly inserted into a porcelain kettle, and then stirred at a temperature of 700°C for 4 hours. 5 g of cooled rice husk ash was dissolved in 30 mL of 2 M NaOH and stirred using a magnetic stirrer at 90°C for 1 hour. Then, the solution was filtered and separated from the residue. The filtrate was isolated by reacting with 37% HCl solution and then shaken to pH 7.

2.3.   Extraction of Calcium Carbonate

As much as 4 g of limestone, which had been crushed into a 200-mesh size, was dissolved using 100 mL of 0.8 M HNO_3 and stirred using a magnetic stirrer for 30 minutes. The solution was then filtered with Whatman 42 filter paper to separate it from impurities. The filtrate was added with 20 mL of 25% NH_3 to make the atmosphere alkaline. The process was continued by CO_2 carbonation using a 3 mm nozzle for 60 minutes and sonicated for 60 minutes from the precipitate to uniform the size. The precipitated calcium carbonate was washed with deionized water until neutral and dried in the oven.

2.4.   Synthesis of WMTA

WMTA was synthesized using the sol-gel process, which started with the dissolution of 10 g of precipitation calcium carbonate (PCC) from limestone in 40 mL of distilled water, followed by adding 0.25 mL of NH_3 for 5

minutes to generate solution I. Solution II was prepared by dissolving 2 g of silica in 30 mL of distilled water, which was then added to 0.25 mL of NH_3 for 5 minutes. Solution III was prepared by dissolving 0.2 g of Al_2O_3 with 0.5 mL of NH_3. The three solutions were mixed and then stirred using a magnetic stirrer for 60 minutes at a speed of 750 rpm. Stirring was continued, accompanied by heating at 85°C for 24 hours for the homogenization process. Then, a thick MTA gel was produced. The MTA gel was dried at 120°C for 6 hours to create a white powder product. The white powder was then given a thermal treatment at a temperature of 1000°C for 3 hours, and the final product was added 18% Bi_2O_3.

3.   Results and Discussion

3.1.   Silica Extraction

The Fourier-transform Infrared Spectroscopy (FTIR) spectra in Figure 1(a) show that the absorptions at 3448 cm⁻¹ and 3441 cm⁻¹ are a water molecule, representing −OH stretching vibration of silanol or water molecules adsorption on the silica surface [10]. Absorption at wavenumber 1650 cm⁻¹ appears in the spectra for all samples. According to Abou Abou Rida and Harb [11], absorption is a bending vibration of water trapped in the silica matrix. This absorption is not entirely lost by heating, but its intensity can be reduced [11].

According to Mujiyanti et al. [12], the SiO_2 character of the absorption bands that appeared in the silica gel spectra generally indicated that the functional groups present in the silica gel made from rice husk ash were silanol groups (Si-OH) and siloxane groups (Si-O-Si), giving vibrations stretching and bending that can be observed at 400-1400 cm⁻¹. In Figure 1, the bands at 1095 cm⁻¹ and 1103 cm⁻¹ are assigned to the vibration absorption of Si-O-Si [13]. The Si-O-Si absorption peak gradually shifts towards high frequency, indicating the stronger band between silicon and oxygen and the higher degree of polymerization of the Si-O-Si groups [14].
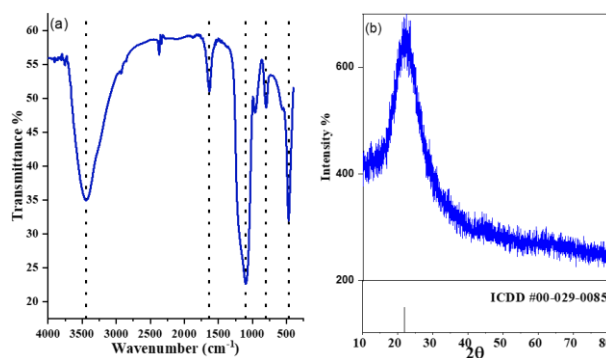

Figure 1. (a) FTIR spectra, (b) XRD diffractograms of silica and ICCD silica
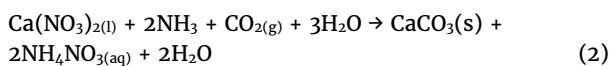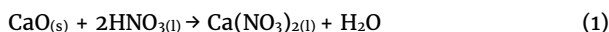
Silica was characterized using X-ray Diffraction (XRD) to identify the level of crystallinity and phases formed from silica. The extracted silica diffractogram that is formed can be seen in Figure 1(b) has a distinctive widened peak at $2\theta = 22°$ and indicates the presence of amorphous silica [15]. According to Bakar et al. [16], optimizing temperature in ash formation can inhibit silica crystallization formation. The phase formed was

amorphous according to ICDD #00-029-0085, and the formed phase was amorphous according to ICDD #00-029-0085, based on Figure 1(b). it can be concluded that silica extraction from rice husk ash was successful.

3.2. Characterization of Calcium Carbonate from Limestone

The spectra (peaks) in the range of wavenumbers 4000-400 cm^{-1} are shown in Figure 2(a). FTIR spectra analysis of calcium carbonate shows the presence of several absorption bands (peaks). The presence of water (-OH functional group) appears at 3448 cm^{-1}. The absorption at 2515 cm^{-1} is assigned to the vibration of the asymmetric C=O functional group [17]. According to Hughes *et al.* [18], a wavenumber of 1419 cm^{-1} is characteristic of the calcite phase. Alam and Chowdhury [19] stated that wavenumbers 871 cm^{-1} and 709 cm^{-1} came from the C-O functional group, which indicated the presence of $CaCO_3$. The functional groups found in calcium carbonate are dominated by C-O bonds.

The diffractogram in Figure 2(b) shows the presence of a calcite phase of $CaCO_3$ according to ICDD #00-005-0586, which has a rhombohedral system; meanwhile, the $CaCO_3$ structure has a calcite shape. This happened because, during extraction using 1 M HNO_3, the concentration of HNO_3 affected the formation of the $CaCO_3$ crystalline phase. The greater the concentration of HNO_3, the greater the tendency to increase the formation of amorphous $CaCO_3$. There is a strong interaction between H^+, OH^-, and Ca^{2+}, which affects the morphology of crystal growth and the formation of $CaCO_3$ particles.

$$CaO_{(s)} + 2HNO_{3(l)} \rightarrow Ca(NO_3)_{2(l)} + H_2O \quad (1)$$

$$Ca(NO_3)_{2(l)} + 2NH_3 + CO_{2(g)} + 3H_2O \rightarrow CaCO_3(s) + 2NH_4NO_{3(aq)} + 2H_2O \quad (2)$$

In Figure 2 (b), it can be seen that the maximum diffraction peak occurs at 2θ = 29.37°. This indicates that the resulting crystals are calcite. The calcium atom is in the face-centered cell of the rhombohedral unit. Calcite has a Miller index of 104 and a diffraction angle of 29.5°, aragonite 221 at 2θ= 47°, and vaterite 110 at 2θ= 25°. In addition, the supporting peaks of the diffraction angle are at 23.02°, 35.97°, 39.57°, 43.66°, 46.04°, 47.58°, 48.50°, 56.66°, and 57.51°. This value is the same as that obtained by ICDD #00-005-0586.
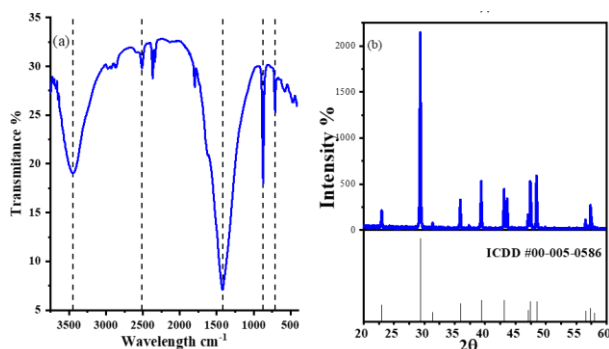

Figure 2. (a) FTIR spectra and (b) XRD diffractogram of Calcium carbonate

3.3. Characterization of WMTA

3.3.1. Decomposition of WMTA

WMTA as a starting material (pre-calcination material) was characterized using TGA to determine sample reduction and thermal stability on heating. WMTA precursors were prepared using 2 g of silica, 10.71 g of calcium carbonate, and 0.2 g of Al_2O_3. The results show a relationship curve between weight vs. temperature (Figure 3(a)). TGA with a testing temperature of 37–1000°C decreased sample weight caused by water loss in WMTA. WMTA with NH_4OH in the area of 550–750°C a decomposition of 3.97 mg occurred, indicating a change in the phase or structure of the compound from $CaCO_3$ to CaO by releasing CO_2 [20]. Characterization DSC (Differential Scanning Calorimetry) was used to evaluate the heat's effect on the phase transitions and chemical reactions in Figure 3(b). The heat rate of experiencing heat release at a temperature of 200°C the loss of water content due to the process, at 750°C shows the highest temperature of a component so that it slows down decomposition as well as phase formation, and at 1000°C the end of the formation of aggregate components so that the graph starts to slope and decline.
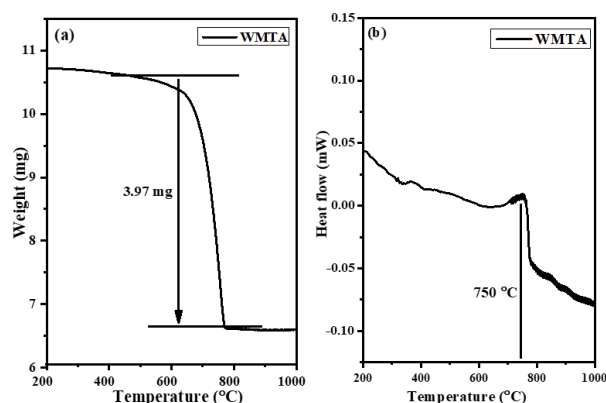

Figure 3. (a) TGA and (b) DSC of MTA

Based on the results of the characteristics of TGA/DSC with a testing temperature of 37–1000°C, it can already form various new phases, especially in the decomposition of $CaCO_3$. The results of XRD characterization can prove this statement after the calcination treatment gives the formation phase, especially the phase involving the decomposition of Ca, which will form Ca_2SiO_4, Ca_3SiO_5, dan $Ca_3Al_2O_6$ with mechanisms (3 to 6).

$$CaCO_3 + SiO_2 \rightarrow CaSiO_3 + CO_2 \quad (3)$$

$$2CaCO_3 + SiO_2 \rightarrow Ca_2SiO_4 + 2CO_2 \quad (4)$$

$$3CaCO_3 + 2SiO_2 \rightarrow Ca_3SiO_5 + 3CO_2 \quad (5)$$

$$3CaCO_3 + Al_2O_3 \rightarrow Ca_3Al_2O_6 + 3CO_2 \quad (6)$$

3.3.2. Structure Characterization and Crystallinity

FTIR characterization was used to compare the presence of functional groups in the WMTA synthesized after calcination at 1000°C. In Figure 4 (left), a wavenumber of 733 cm^{-1} is seen in the IR spectra, which indicates the presence of Si-O [21]. In this process,

silanol Si-OH groups were also obtained at 1055 cm^{-1}. In addition, there are also O-H groups that indicate water molecules at 3140 cm^{-1}.

MTA has a sharp absorption at 3360 cm^{-1}, showing the vibration of the −OH group of Ca(OH)$_2$ formed. The wavenumber of 3140 cm^{-1} appears the same as the weaker WMTA spectra, indicating a decrease in the −OH functional group. In addition, in WMTA, after calcination, Si-O vibrations appeared at 1110 cm^{-1} and 623 cm^{-1} from the Si-O functional groups indicating the presence of Si-O-Ca bonds [22].

WMTA is similar to ProRoot, after calcining the powder at a temperature of 1000°C, adding bismuth oxide at the end of the reaction, and changing the functional group Ca(OH)$_2$ to Si-O-Ca at 874 cm^{-1}. The characteristic spectral peaks of silica on WMTA tend to change after this calcination. Calcination resulted in a widened absorption. Based on this statement, it can be indicated that there has been a reaction between Si and other compounds to produce characteristic absorption bands such as WMTA ProRoot. Bi$_2$O$_3$ absorption as a radiopaque agent in WMTA can be seen at wave numbers < 600 cm^{-1} [23]. Research that supports Bi$_2$O$_3$ absorption at this wave number is Indurkar *et al.* [24], in the form of Bi-O bending vibrations. The experimental results showed uptake of Bi-O at 516 cm^{-1} for all treatments. The absorption also overlaps with the absorption of SiO$_2$ formation. Another indication can be revealed that SiO$_2$ has changed into another phase. Then the wavenumber originally occupied by SiO$_2$ is absorbed by Bi$_2$O$_3$ [24].
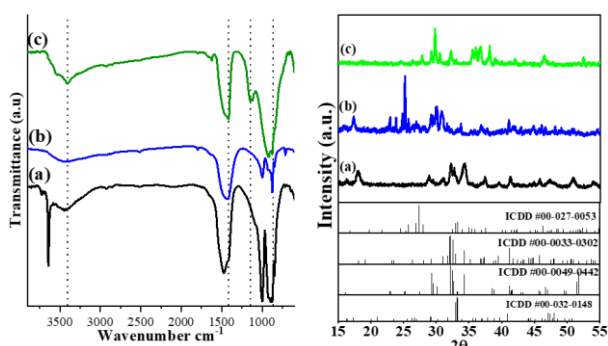

Figure 4. FTIR (left) and XRD (right) of (a) MTA (b) WMTA (c) ProRoot

Characterization by XRD to determine the structure and crystallinity of WMTA treated WMTA powder after calcining at 1000°C and adding bismuth oxide at the end of the reaction. The resulting product was characterized by its crystallinity, and the results are shown in Figure 4 (right). The figure shows that WMTA has been successfully synthesized because it has a peak similar to ProRoot. In each sample, the Bi$_2$O$_3$ phase ICDD #00-027-0053 has a monoclinic crystal system, tricalcium silicate (Ca$_3$SiO$_5$, C$_3$S) ICDD #00-0033-0302 has a monoclinic crystal system and dicalcium silicate (Ca$_2$SiO$_4$, C$_2$S) ICDD #00 -0049-0442 has a monoclinic crystal system and tricalcium aluminate phase (Ca$_3$Al$_2$O$_6$) ICDD #00-032-0148 has a monoclinic system. The XRD results which are characteristic of WMTA are the appearance of the characteristic peak of Bi$_2$O$_3$ at 2θ = 24.62°, 25.82°, 27.34°, 28.30°, and 46.32°, tricalcium silicate crystals at 2θ = 32.53°, 34.13°, 52.32°, and the dicalcium silicate phase at 2θ = 18.26°, 32.13°, 37.52°, 41.22°, 50.81° and tricalcium aluminate phase 2θ = 33.24°.

Characterization by XRD of WMTA samples which can be seen in Figure 4 (right), shows that the crystallinity of each sample is similar to WMTA ProRoot. The intensity associated with Ca$_2$SiO$_4$ at 2θ = 17.94° is due to the NH$_3$ used as a catalyst in the sol-gel process affecting the peak intensity [25, 26]. Tricalcium silicate is the main component in forming calcium silicate hydrate, which provides initial strength for physical properties. Alumina silicate is the most reactive element and reacts quickly with water. However, its contribution to the physical strength of WMTA is minimal [24]. The alumina silicate phase is produced by adding alumina to the mix, and alumina helps to reduce the firing temperature used to form WMTA cement [27]. The intensity of the peaks is nearly similar to WMTA ProRoot. It shows similarities in the important peaks, Ca$_3$SiO$_5$ and Ca$_2$SiO$_4$, at the 2θ = 30-35°.

3.3.3. SEM Analysis

The MTA, WMTA, and ProRoot images are presented in Figure 5. In these images with a magnification of 5000×, it is visible that calcined MTA has a uniform morphology as if covered by granular material. The WMTA image from the experimental results can be seen in Figure 5. The synthesized WMTA has a morphology with a uniform particle shape. This indicates that the WMTA experimental results have a homogeneous structure. ProRoot is a commercial WMTA that has a uniform morphology.
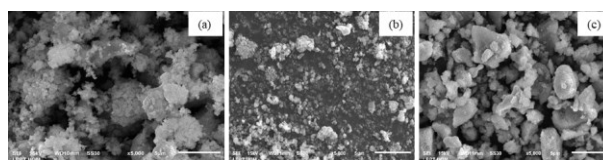

Figure 5. SEM images of (a) MTA (b) WMTA (c) ProRoot

3.3.4. Radiopacity

In dentistry, radiographic examination of endodontic materials has a role in determining radiopaque properties. The experimental WMTA used Bi$_2$O$_3$, giving WMTA radiopaque properties according to WMTA ProRoot [25].
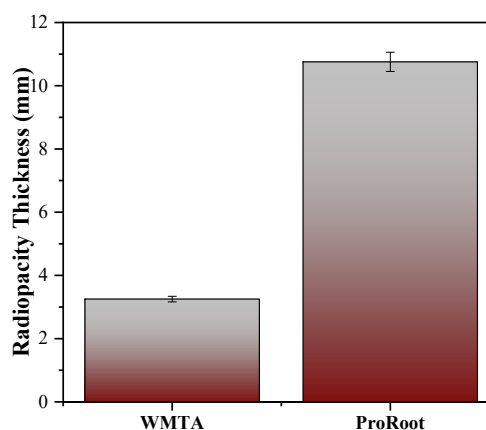

Figure 6. Table of Radiopacity WMTA and ProRoot

The standard for assessing the radiopacity of materials used radiographic films according to ISO 4049 standards. WMTA has a radiopacity value of 3 mm Al, which can distinguish between WMTA and teeth during the treatment process. The results of the radiopacity test are presented in Figure 6. WMTA ProRoot has the highest radiopaque value of 10.76 ± 0.305 mm. However, the synthesis results show that the WMTA is only 3.250 ± 0.088 mm.

4. Conclusion

The silica of rice husk ash and calcium carbonate produced has the potential as a base material for WMTA. Silica was successfully extracted from rice husk ash. Calcium carbonate can be synthesized by the carbonation method by adding HNO_3. WMTA with a temperature of 1000°C was successfully synthesized, having Ca_3SiO_5, Ca_2SiO_4, and $Ca_3Al_2O_6$ phases similar to WMTA ProRoot. Radiopacity value of WMTA 3.250 ± 0.088 mm.

References

[1] G. Voicu, A. I. Bădănoiu, C. D. Ghiţulică, E. Andronescu, Sol-gel synthesis of white mineral trioxide aggregate with potential use as biocement, *Digest Journal of Nanomaterials and Biostructures*, 7, 4, (2012), 1639–1646

[2] Gul Celik Unal, Murat Maden, Tugba Isidan, Repair of furcal iatrogenic perforation with mineral trioxide aggregate: two years follow-up of two cases, *European Journal of Dentistry*, 4, 4, (2010), 475–481

[3] Camila Corral-Núñez, Eduardo Fernández-Godoy, Javier Martín Casielles, Juan Estay, Cristian Bersezio-Miranda, Patricia Cisternas-Pinto, Osmir Batista Batista-de Oliveira, Current state of calcium silicate cements in restorative dentistry: a review, *Revista Facultad de Odontología Universidad de Antioquia*, 27, 2, (2016), 425–441 https://doi.org/10.17533/udea.rfo.v27n2a10

[4] R. Steffen, H. van Waes, Understanding mineral trioxide aggregate/Portlandcement: a review of literature and background factors, *European Archives of Paediatric Dentistry*, 10, (2009), 93–97 https://doi.org/10.1007/BF03321608

[5] Robert K. Murray, *Biokimia Harper*, 25 ed., EGC, Jakarta, 2001

[6] Mahmoud Torabinejad, Chan-Ui Hong, Seung-Jong Lee, Mehdi Monsef, Thomas R. Pitt Ford, Investigation of mineral trioxide aggregate for root-end filling in dogs, *Journal of Endodontics*, 21, 12, (1995), 603–608 https://doi.org/10.1016/S0099-2399(06)81112-X

[7] Muchtar Aziz, Batu kapur dan peningkatan nilai tambah serta spesifikasi untuk industri, *Jurnal Teknologi Mineral dan Batubara*, 6, 3, (2010), 116–131

[8] Mita Wulandari Lukman, Sintesis Biomaterial Komposit CaO-SiO₂ Berbasis Material Alam (Batuan Kapur dan Pasir Kuarsa) dengan Variasi Suhu Pemanasan dan Pengaruhnya Terhadap Porositas, Kekerasan dan Mikrostruktur, Journal Sains, Univesitas Negeri Malang, Malang, 2012

[9] Abhisk Mehta, R. P. Ugwekar, Extraction of silica and other related products from rice husk, *International Journal of Engineering Research and Applications*, 5, 8, (2015), 43–48

[10] Suyanta Suyanta, Agus Kuncaka, Utilization of rice husk as raw material in synthesis of mesoporous silicates MCM-41, *Indonesian Journal of Chemistry*, 11, 3, (2011), 279–284 https://doi.org/10.22146/ijc.21393

[11] Maurice Abou Abou Rida, Faouzi Harb, Synthesis and characterization of amorphous silica nanoparitcles from aqueous silicates uisng cationic surfactants, *Journal of Metals, Materials and Minerals*, 24, 1, (2014), 37–42

[12] Dwi Rasy Mujiyanti, Nuryono Nuryono, Eko Sri Kunarti, Sintesis dan karakterisasi silika gel dari abu sekam padi yang diimobilisasi dengan 3-(trimetoksisilil)-1-propantiol, *Jurnal Berkala Ilmiah Sains dan Terapan Kimia*, 4, 2, (2010), 150–167

[13] S. Azat, A. V. Korobeinyk, K. Moustakas, V. J. Inglezakis, Sustainable production of pure silica from rice husk waste in Kazakhstan, *Journal of Cleaner Production*, 217, (2019), 352–359 https://doi.org/10.1016/j.jclepro.2019.01.142

[14] Hervé Kouamo Tchakouté, Claus Henning Rüscher, Sakeo Kong, Navid Ranjbar, Synthesis of sodium waterglass from white rice husk ash as an activator to produce metakaolin-based geopolymer cements, *Journal of Building Engineering*, 6, (2016), 252–261 https://doi.org/10.1016/j.jobe.2016.04.007

[15] José Arnaldo Santana Costa, Caio Marcio Paranhos, Systematic evaluation of amorphous silica production from rice husk ashes, *Journal of Cleaner Production*, 192, (2018), 688–697 https://doi.org/10.1016/j.jclepro.2018.05.028

[16] Rohani Abu Bakar, Rosiyah Yahya, Seng Neon Gan, Production of high purity amorphous silica from rice husk, *Procedia Chemistry*, 19, (2016), 189–195 https://doi.org/10.1016/j.proche.2016.03.092

[17] Noviyanti Noviyanti, Jasruddin Jasruddin, Eko Hadi Sujiono, Karakterisasi kalsium karbonat (Ca(CO₃)) dari batu kapur kelurahan Tellu Limpoe kecamatan Suppa, *Jurnal Sains dan Pendidikan Fisika*, 11, 2, (2015), 169–172

[18] Trevor L. Hughes, Claire M. Methven, Timothy G. J. Jones, Sarah E. Pelham, Philip Fletcher, Christopher Hall, Determining cement composition by Fourier transform infrared spectroscopy, *Advanced Cement Based Materials*, 2, 3, (1995), 91–104 https://doi.org/10.1016/1065-7355(94)00031-X

[19] Md Shahinoor Alam, Mohammad Asaduzzaman Chowdhury, Characterization of epoxy composites reinforced with CaCO₃-Al₂O₃-MgO-TiO₂/CuO filler materials, *Alexandria Engineering Journal*, 59, 6, (2020), 4121–4137 https://doi.org/10.1016/j.aej.2020.07.017

[20] Georgeta Voicu, Alina Bădănoiu, Ecaterina Andronescu, Carmen Chifiruc, Synthesis, characterization and bioevaluation of partially stabilized cements for medical applications, *Central European Journal of Chemistry*, 11, (2013), 1657–1667 https://doi.org/10.2478/s11532-013-0297-1

[21] Warda Ashraf, Jan Olek, Vahit Atakan, A comparative study of the reactivity of calcium silicates during hydration and carbonation

reactions, *14th International Congress on the Chemistry of Cement (ICCC 2015)*, Beijing, China, 2015

[22] Anikó Meiszterics, László Rosta, Herwig Peterlik, János Rohonczy, Shiro Kubuki, Péter Henits, Katalin Sinkó, Structural characterization of gel-derived calcium silicate systems, *The Journal of Physical Chemistry A*, 114, 38, (2010), 10403-10411 https://doi.org/10.1021/jp1053502

[23] Wen-Hsi Wang, Chen-Ying Wang, Yow-Chyun Shyu, Cheing-Meei Liu, Feng-Huei Lin, Chun-Pin Lin, Compositional characteristics and hydration behavior of mineral trioxide aggregates, *Journal of Dental Sciences*, 5, 2, (2010), 53-59 https://doi.org/10.1016/S1991-7902(10)60009-8

[24] Abhishek R. Indurkar, Viraj D. Sangoi, Prashant B. Patil, Mansingraj S. Nimbalkar, Rapid synthesis of Bi_2O_3 nano-needles via 'green route' and evaluation of its anti-fungal activity, *IET Nanobiotechnology*, 12, 4, (2018), 496-499 https://doi.org/10.1049/iet-nbt.2017.0070

[25] Saeed Asgary, Mohammad Jafar Eghbal, Masoud Parirokh, Jamileh Ghoddusi, Sanam Kheirieh, Frank Brink, Comparison of mineral trioxide aggregate's composition with Portland cements and a new endodontic cement, *Journal of Endodontics*, 35, 2, (2009), 243-250 https://doi.org/10.1016/j.joen.2008.10.026

[26] Steven Gu, Brian J. Rasimick, Allan S. Deutsch, Barry Lee Musikant, Radiopacity of dental materials using a digital X-ray system, *Dental Materials*, 22, 8, (2006), 765-770 https://doi.org/10.1016/j.dental.2005.11.004

[27] Irma Araceli Belío-Reyes, Lauro Bucio, Esther Cruz-Chavez, Phase composition of ProRoot mineral trioxide aggregate by X-ray powder diffraction, *Journal of Endodontics*, 35, 6, (2009), 875-878 https://doi.org/10.1016/j.joen.2009.03.004